Counteranion-dependent mechanisms of intramolecular proton transfer in aprotic solution†

Stepan B. Lesnichin,[ab] Peter M. Tolstoy,[ab] Hans-Heinrich Limbach[b] and Ilja G. Shenderovich*[ab]

Received 19th March 2010, Accepted 28th April 2010
DOI: 10.1039/c004499g

Using the freon mixture $CDF_3/CDClF_2$ as solvent we have been able to measure the ^1H and ^{15}N NMR spectra of the doubly ^{15}N labeled 2,2′-bipyridinium cation ($BpyH^+$) at temperatures down to 115 K. The obtained NMR parameters strongly depend on the type of counteranions indicating the formation of ion pairs. In the case of the bulky poorly coordinating tetrakis[3,5-bis(trifluoromethyl)phenyl]-borate as the counteranion a strong intramolecular NHN hydrogen bond was observed in $BpyH^+$ exhibiting a degenerate intramolecular proton transfer which is of the order of 10^6 s^{-1} even at 120 K. By contrast, the weak hydrogen bond acceptor tetrafluoroborate favors a weak intermolecular FHN interaction and quenches the intramolecular proton transfer. The intramolecular proton transfer requires in this case a dissociation of the ion pair which is hindered by the Coulomb interaction. A slow intramolecular proton transfer was observed in the case of dichloroacetate which forms a strong intermolecular OHN hydrogen bond to $BpyH^+$. The mechanism of this transfer presumably involves a preliminary intermolecular proton transfer from nitrogen towards oxygen followed by a hydrogen bond switch to the neighboring nitrogen to which the proton is then transferred.

Introduction

Proton transport is a part of many biological processes.[1] Although only a single elementary particle is displaced, the process can take place *via* many different reaction mechanisms that depend both on the reacting molecules and the medium.[2] The understanding of the nature of proton transfer in biological systems requires the identification of the possible mechanisms using small, well-defined molecular systems.

NMR spectroscopy using ^{15}N as a nuclear probe can cover a dynamic range of various proton transfers from and to nitrogen from the millisecond to the nanosecond timescale. Some characteristic examples are depicted in Scheme 1. Resonance-assisted transfers are possible in neutral molecules such as *N*,*N*′-diphenyl-6-aminofulvene-1-aldimine (Scheme 1a).[3] Generally, there are little liquid–solid state effects on the reaction dynamics in such systems. When proton transfer in neutral molecules involves zwitterionic intermediates or transition states, the influence of the environment can become important. An example is the base-catalyzed tautomerism of diaryl-triazenes (Scheme 1b).[4] Although stronger effects are expected in charged systems, the migrating proton can be well shielded from the counterion. Porphyrin anion (Scheme 1c) exhibits no dependence on the environment.[5] In other systems the proton localization can be effected by counterions or solvent molecules. An example is the homoconjugated cation of 2,4,6-trimethyl-pyridine (Scheme 1d).[6] In this case the potential surface of the bridging proton has two minima separated by a low barrier through/above which the proton transfer process can occur.[7] In the crystalline state the geometries of hydrogen bonds in homoconjugated ions depend on specific interactions between cation and anion. Here the proton transfer would require a reorganization of the crystal structure. In contrast, in aprotic solvents a fast dynamic equilibrium (Scheme 1d) has been observed even at temperature down to 100 K.[6] The driving forces initiating proton jumps are fluctuations of the counterion positions and/or of the external electric field produced by solvent molecules. The same effects have been observed for the intramolecular NHN hydrogen bonds of protonated sponges of the 1,8-*N*,*N*′-diaminonaphthalene type (Scheme 1e).[8]

However, in the listed charged systems the hydrogen bonds are sterically hindered. Thus, they are not suitable to inspect characteristic features of their interactions with a certain counterion.

Therefore, we have performed low-temperature NMR experiments on the monoprotonated cation 2,2′-bipyridinium ($BpyH^+$) (Scheme 2). In contrast to the homoconjugated pyridine cations and protonated sponges the interaction of the mobile proton of $BpyH^+$ with the anion is not affected by the molecular structure of the cation. Here, the effect of cation–anion interactions on the intramolecular tautomerism according to Scheme 2b can be studied using the doubly ^{15}N labeled compound. Naturally, a *cis*-conformation is required for the formation of an intramolecular NHN hydrogen bond. Indeed, X-ray structure analysis indicates that $BpyH^+$ ClO_4^- crystallizes in the *cis*-conformation, exhibiting a non-linear NHN-hydrogen bond where the proton is localized in an asymmetric position close to one of the two nitrogen atoms

[a] *Institut für Chemie und Biochemie der Freien Universiät Berlin, Takustrasse 3, D-14195, Berlin, Germany. E-mail: shender@chemie.fu-berlin.de; Fax: +49 30 83855310; Tel: +49 30 83853615*
[b] *Institute of Physics, St. Petersburg State University, 198504, St. Petersburg, Russia*

† Electronic supplementary information (ESI) available: Detailed description of the synthesis of ^{15}N labeled 2,2'-bipyridine. See DOI: 10.1039/c004499g

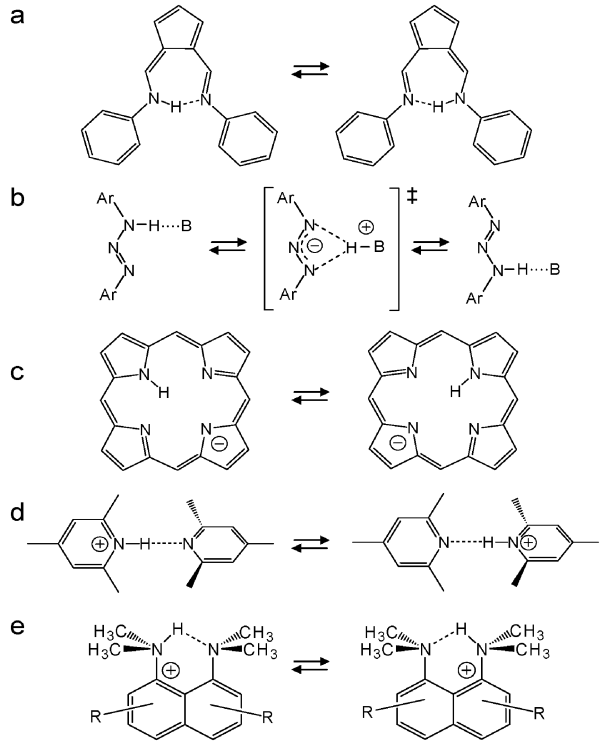

Scheme 1 Degenerate proton transfers in NHN hydrogen bonds.

which are 2.75 Å apart from each other.[9] Apparently, the interaction with the anion blocks the intramolecular proton transfer in the solid. By contrast, in the absence of specific interactions crystalline Bpy exhibits a planar *trans*-conformation (Scheme 2a).[10] Theoretical calculations estimate the stabilization energy of the *trans*- as compared to the *cis*-conformer as 6 kJ mol^{-1}.[11]

In contrast to the solid state, the intramolecular tautomerism of $BpyH^+$ could occur in the liquid state. As a result of the overview on degenerate proton transfer from and to nitrogen presented in Scheme 1, one can conceive several proton transfer mechanisms. Scheme 3a depicts the case where the counteranion does not lead to a preference of one of the tautomers. This situation is typical for polar solvents where the ion pair is dissociated or if the electrical charge of the anion is well shielded.[12] Proton transfer requires in both cases only solvent reorganization. In Scheme 3b a hydrogen bond of medium strength is formed between cation and anion. This contact ion pair needs to dissociate before proton transfer can occur along a weak intramolecular hydrogen bond. Finally, in Scheme 3c a contact ion pair exhibiting a strong hydrogen bond is formed. Here, the proton can be first transferred to the

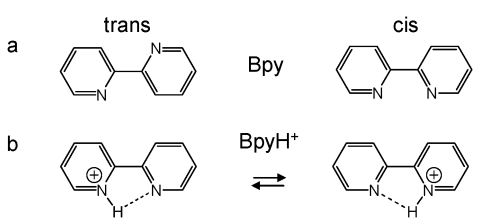

Scheme 2 Chemical structure and conformation of (a) 2,2′-bipyridine (Bpy) and (b) 2,2′-bipyridinium ($BpyH^+$).

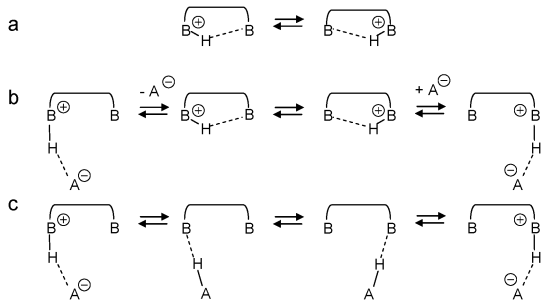

Scheme 3 Mechanisms of intramolecular proton transfer in cationic species in the presence of a counteranion.

anion followed by a hydrogen bond switch.[13] Finally, the proton is transferred back to the acceptor.

In order to explore the different pathways we have studied $BpyH^+$ in the presence of the counteranions depicted in Scheme 4. In the weakly interacting bulky tetrakis[3,5-bis-(trifluoromethyl)phenyl] borate ($BARF^-$) the electrical charge is well shielded.[12] Tetrafluoroborate (BF_4^-) is a weak hydrogen bond acceptor exhibiting some charge delocalization.[14] Dichloroacetate (AC^-) represents a strong hydrogen bond acceptor, especially for protonated pyridines.[15] The polar freon mixture $CDF_3/CDClF_2$ was used as solvent as it is liquid down to 100 K and allows one to observe hydrogen bonded complexes in the slow exchange regime.[16]

This paper is organized as follows. After an experimental section the results of the low-temperature NMR experiments on $BpyH^+$ in $CDF_3/CDClF_2$ in the presence of $BARF^-$, BF_4^- and AC^- are described and discussed.

Experimental

Materials

All chemicals were purchased from Sigma-Aldrich and used without additional purification. Deuterated solvents were purchased from Eurisotop (Germany). The deuterated freon gas mixture $CDF_3/CDClF_2$ for the low-temperature NMR experiments, whose composition varied between 1 : 2 and 1 : 3, was prepared from chloroform-d_1 as described recently.[16]

Preparation of ^{15}N labeled bipyridine. 2,2′-bi-^{15}N-pyridine was synthesized using a procedure adjusted to ^{15}N labeled NH_4Cl as the starting material.[17] The detailed procedure is described in the ESI.†

Preparation of $BpyH^+$-$CHCl_2COO^-$ and $BpyH^+$-BF_4^-. 15.4 mg of 2,2′-bi-^{15}N-pyridine and 12.9 mg of dichloroacetic

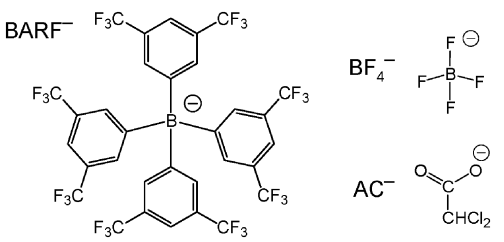

Scheme 4 Counteranions used in this study.

acid (or 17.6 mg 50% aqueous solution of tetrafluoroboric acid) were dissolved in 2 ml of dichloromethane and stirred over 2 h at room temperature. The solvent was removed by rotary evaporation leaving a white salt. The salt was dried overnight under vacuum.

Preparation of BpyH$^+$-BARF$^-$. 15.4 mg of 2,2′-bi-^{15}N-pyridine and 12.9 mg of 37% HCl water solution were dissolved in 2 ml of water by stirring at room temperature. After 15 min 88.6 mg of yellowish Na$^+$ [BARF]$^-$ powder was added. The mixture was stirred over 5 h at room temperature. The white flakes of BpyH$^+$–BARF$^-$ were filtered out and washed with water. The salt was dried overnight under high vacuum.

The purity of the products and the base/acid ratio were inspected by ^{1}H and ^{15}N NMR.

NMR experiments

Liquid-state ^{1}H and ^{15}N NMR spectra were measured on a Bruker AMX 500 spectrometer (500.13 MHz for ^{1}H, 50.68 MHz for ^{15}N) equipped with a low-temperature probe-head enabled to perform experiments down to 100 K. A liquefied deuterated freon gas mixture $CDF_3/CDClF_2$ was used as a solvent. The ^{1}H spectra were indirectly referenced to tetramethylsilane (TMS) by setting the central component of the residual $CHClF_2$ triplet of the freon mixture to 7.18 ppm.[16] The ^{15}N spectra were indirectly referenced to bipyridine dissolved in $CDF_3/CDClF_2$ which resonates at 281 ppm with respect to external solid $^{15}NH_4Cl$ and at −60 ppm with respect to external liquid nitromethane if the following relation $\delta(CH_3{}^{15}NO_2,\ \text{liq.}) = \delta(^{15}NH_4Cl,\ \text{solid})$—341.168 ppm[18] is taken into account.

The standard ^{1}H and ^{15}N NMR spectra were recorded with recycle times of 3 and 5 s, respectively. Dynamic NMR 7.1 code was used for the line-shape analysis of ^{1}H spectra.[19]

NMR lineshape analyses

The ^{1}H NMR line shapes of a proton jumping from and to ^{15}N nuclei can provide information about the proton transfer rate constants as well as on the reaction pathway.[20] In the slow exchange regime the proton signal of a $^{15}NH^{15}N$ hydrogen bond exhibits a scalar coupling to the ^{15}N nucleus to which it is attached, characterized by the coupling constant $^1J(^{15}N,^1H) \equiv J_{NH}$. If we neglect scalar coupling across the hydrogen bond to the other ^{15}N nucleus—a phenomenon which arises only in strong NHN hydrogen bonds[21]—the mobile proton signal will be split into a doublet. The onset of intermolecular proton exchange will broaden the lines of the doublet which coalesce and sharpen again into a singlet. The line shape can be calculated in terms of the usual degenerate two-state exchange theory.[20] By contrast, an intramolecular transfer leads to a doublet–triplet transition. When both intra- and intermolecular proton transfers are superimposed, a broadened triplet may be observed before the scalar coupling disappears.

As an example, we have plotted in Fig. 1 the line shape of the mobile proton in the presence of a degenerate intramolecular proton transfer between two ^{15}N nuclei as a function of the rate constant k. We choose a value of J_{NH} = 94 Hz and a value of W_o = 30 Hz for the linewidth in the absence of exchange which are typical of protonated pyridines.[22] In the absence of exchange, when the rate constant k = 0, both values determine entirely the doublet line shape of the ^{1}H signal. When k is increased, each of the two lines broadens, coalesces and sharpens again into a triplet which eventually reaches the peak height ratio of 1 : 2 : 1. The central peak arises from protons jumping between ^{15}N nuclei in different spin states, whereas the two outer lines stem from protons jumping between ^{15}N nuclei in the same spin state. The total line shape can then be simulated in terms of a degenerate two-state exchange theory and two non-exchanging singlets as depicted in Fig. 1.[20] In all cases, k can be obtained without assumptions as J_{NH} and W_o are determined by the line shape of the outer lines.

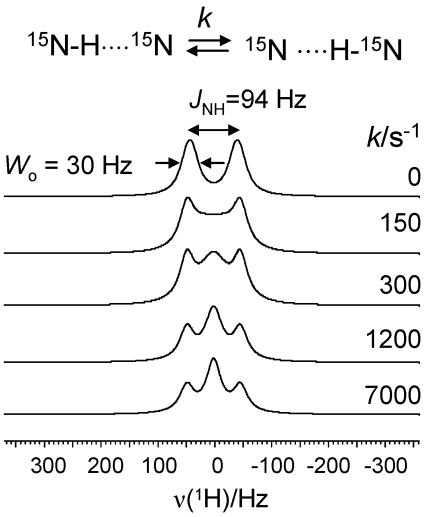

Fig. 1 Simulated ^{1}H NMR signals of an ^{15}N–^{1}H···^{15}N spin system in the presence of an intramolecular degenerate proton transfer characterized by the rate constant k. For further description see text.

Results

Low-temperature ^{1}H NMR spectroscopy

The low-field ^{1}H NMR signals of Bpy/acid complexes in $CDF_3/CDClF_2$ measured at low temperatures are depicted in Fig. 2. The main NMR parameters extracted from the spectra are collected in Table 1. In all cases scalar couplings to ^{15}N are observed indicating the formation of BpyH$^+$ cations. However, the signals depend strongly on the type of the counteranion. In the case of AC$^-$ (Fig. 2a to c), at 115 K a doublet is observed exhibiting a coupling constant J_{NH} = −83 Hz. We assign to the coupling the negative value taking into account the results of theoretical calculations on pyridinium.[23] The signal is shifted to low field when temperature is increased. Concurrently, the doublet is converted into a triplet characterized by a coupling constant of J_{NH} = −40 Hz, at 120 K. This type of transition indicates an intramolecular degenerate proton transfer.[20] At 130 K the signal broadens because of the onset of intermolecular proton exchange[4,20] which leads eventually to loss of the splitting.

By contrast, a doublet observed in the case of BF_4^- does not shift with temperature, and does not exhibit a doublet–triplet

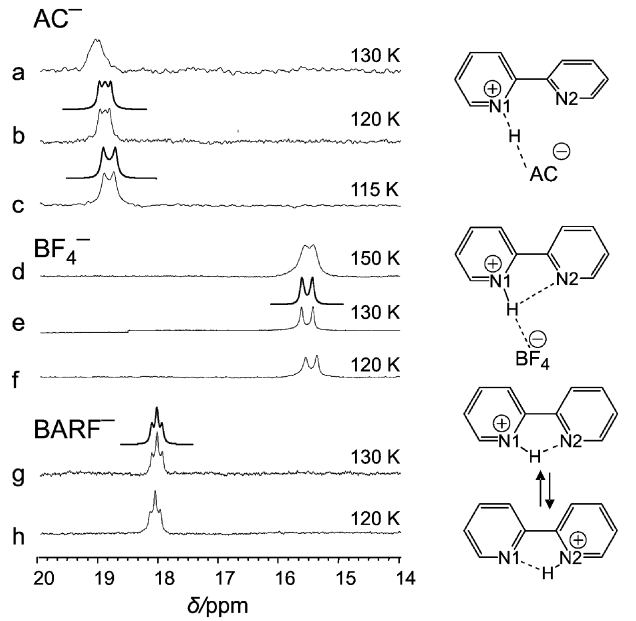

Fig. 2 Low-field low-temperature experimental and simulated ^{1}H NMR signals of $BpyH^{+}$ in $CDF_3/CDClF_2$ in the presence of different counteranions (Scheme 4). The rate constants of the intramolecular proton transfer obtained from the simulated signals are 340 s^{-1} (b); 120 s^{-1} (c); <10 s^{-1} (e); $>10^4$ s^{-1} (g).

transition. When temperature is increased, only a broadening is observed arising from intermolecular proton exchange. The signal broadening at the lowest temperature arises from the increase of the solvent viscosity.

In the case of $BARF^{-}$ as counterion the hydrogen bonded proton of $BpyH^{+}$ is a triplet even at the lowest temperatures. Its chemical shift and multiplicity are also independent of temperature.

Low-temperature ^{15}N NMR spectroscopy

Experimental low-temperature ^{15}N NMR spectra of Bpy and $BpyH^{+}$ dissolved in $CDF_3/CDClF_2$ in the presence of different anions are depicted in Fig. 3. The spectra were obtained in the absence of ^{1}H decoupling. The NMR parameters extracted from these measurements are included in Table 1.

In Fig. 3a the signal of free Bpy is depicted. For convenience we used Bpy as reference in this study and set its chemical shift to 0 ppm.

Table 1 NMR parameters of $BpyH^{+}$ complexes in $CDF_3/CDClF_2$

Complex		T/K	δ (^{1}H)/ppm	δ (^{15}N)/ppm	J_{NH}/Hz
$BpyH^{+}$ AC^{-}	[a]	130	19.1		—
	[a]	120	18.9		-81 ± 3
	[a]	115	18.8	N1: -95	-83 ± 1
				N2: $+2$	
$BpyH^{+}$ BF_4^{-}	[a]	150	15.6		—
	[a]	130	15.6		-94 ± 1
	[a]	120	15.6	N1: -111	-94 ± 1
				N2: -5	
$BpyH^{+}$ $BARF^{-}$	[a]	130	18.0		-42 ± 1
	[a]	120	18.0	N1/N2: -67	-42 ± 2
$ColH^{+}Col$ BF_4^{-}	[b]	150	19.9	N1/N2: -58	-40

[a] This study. [b] Ref. 8. For atom numbering see Fig. 2.

After protonation with dichloroacetic acid two new signals appear. The first signal at -95 ppm exhibits a doublet splitting and, therefore, corresponds to the protonated nitrogen N1. The singlet at $+2$ ppm corresponds to the non-protonated nitrogen N2. This sample contains some free Bpy, the singlet at 0 ppm. In the case of $BpyH^{+}$ BF_4^{-} a similar spectrum is observed, although both signals are shifted to high field. By contrast, only a single doublet is observed in the case of $BARF^{-}$ indicating a fast proton transfer along an intramolecular pathway as shown by the triplet splitting of the corresponding ^{1}H signal.

Discussion

The NMR parameters of doubly ^{15}N labeled bipyridine dissolved in $CDF_3/CDClF_2$ measured at 150 K and below in the presence of three acids indicate that bipyridine is protonated and that ion pairs are formed with the acid anions. The first statement is corroborated by the large coupling constant J_{NH} and the second by the finding of different NMR parameters for the three systems. In the case of dissociated ion pairs the NMR parameters would not depend on the acid used.

For XHN hydrogen bonds (X = O, F, N) analysis of geometric parameters based on neutron structures indicated that the distances XH and HN are correlated with each other. If one distance is known, the other can be estimated using empirical equations.[24] For collidine–carboxylic acid complexes it has been shown by dipolar NMR that their ^{15}N chemical shifts are correlated with the NH distances of the OHN hydrogen bonds.[25] Besides that, for hydrogen bonds of the OHN type involving pyridine there is a correlation between the ^{15}N chemical shift and the ^{1}H chemical shift of the mobile proton.[26]

Structures of the bipyridinium–anion complexes

The values of the chemical shifts and scalar couplings of the $BpyH^{+}$ BF_4^{-} complex are close to the values expected for a

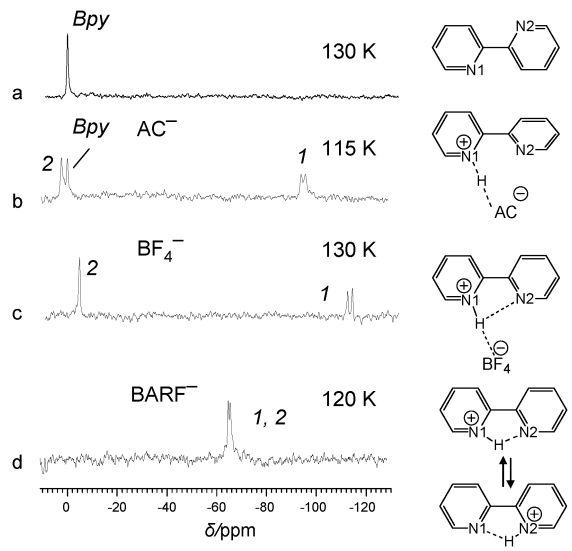

Fig. 3 Low-temperature ^{15}N NMR spectra of $BpyH^{+}$ in $CDF_3/CDClF_2$ in the presence of different counteranions (Scheme 4).

protonated pyridine involved in a weak hydrogen bond.[22] Based on the ^{15}N chemical shift of −111 ppm for the protonated nitrogen atom we can estimate that the NH distance in the $BpyH^+$ BF_4^- complex is about 1.05 Å.[25] The chemical shift value of the non-protonated nitrogen atom is slightly negative. This fact indicates that this nitrogen is involved in a hydrogen bond as well. Indeed, the ^1H chemical shift of 15.6 ppm is characteristic of a hydrogen bond of moderate strength. From these findings it follows that the $BpyH^+$ BF_4^- complex exhibits an asymmetric structure, where the proton is localized on one of the pyridine rings. An intramolecular proton transfer below 150 K is either slow or absent. Above this temperature, intermolecular proton transfer set in. We ascribe the hindrance of the intramolecular proton transfer to the formation of an intermolecular hydrogen bond to the counteranion BF_4^-.

By contrast, intramolecular proton transfer is fast in the $BpyH^+$ $BARF^-$ complex. The intramolecular pathway follows from the observation of the triplet in the ^1H NMR spectrum arising from scalar coupling to both nitrogen atoms of $BpyH^+$. The coupling constant is −42 Hz, indicating an intrinsic coupling of about −84 Hz. This represents a strong decrease as compared to the value found for $BpyH^+$ BF_4^- and corroborates together with the low-field shift to 18 ppm a much stronger hydrogen bond. Only a single averaged ^{15}N signal is observed down to 120 K. This means $BpyH^+$ $BARF^-$ adopts a *cis*-conformation stabilized by the intramolecular hydrogen bond. In order to obtain information about the hydrogen bond geometry the intrinsic ^{15}N chemical shifts of both nitrogen atoms in the slow exchange regime are required. These data can be estimated from the $^1H/^{15}N$ correlation.[26] The ^1H chemical shift of 18 ppm of $BpyH^+$ $BARF^-$ corresponds to a ^{15}N chemical shift of about −100 ppm for the protonated pyridine. This value corresponds to an NH distance of about 1.07 Å. From the NHN hydrogen bond correlation we then estimate the second NH distance to be about 1.7 Å. A similar estimation for the related homoconjugated 2,4,6-trimethylpyridine cation $ColH^+Col$ BF_4^- (Scheme 1d, Table 1)[6] leads to the NH distances of 1.1 and 1.6 Å, correspondingly. Thus, the NHN hydrogen bond in the $BpyH^+$ $BARF^-$ complex is less strong than that of the $ColH^+Col$ BF_4^-. We also note that BF_4^- does not hinder the intramolecular proton transfer in $ColH^+Col$.

Finally, the ^{15}N chemical shifts of the $BpyH^+$ AC^- complex indicate a short NH distance of 1.1 Å. As the non-protonated nitrogen N2 resonates at +2 ppm this atom is not involved in a hydrogen bond. The chemical shift of the hydrogen bond proton, 19 ppm, and the reduced $^1H^{15}N$ coupling constant of −81 Hz attest the formation of a strong OHN hydrogen bond to AC^-. From the corresponding correlation it follows that the H···O distance is about 1.45 Å. This also explains the fact that the mobile proton exhibits the largest chemical shift of the three complexes. Of course, the values of the proton chemical shift depend on the molecules forming the hydrogen bond and cannot be compared for very different systems.[27] However, in the discussing complexes the mobile protons are already transferred to $BpyH^+$ and in the first approximation the numerical values of the ^1H resonance depend only on the N···H distance. As temperature is increased the proton signal of the $BpyH^+$ AC^- complex is shifted to low field. As the dielectric constant of the freon mixture is decreased at the same time (45 at 100 K to 25 at 145 K)[16] this means that the proton is shifted towards the hydrogen bond center, a typical effect for zwitterionic hydrogen bonds. This shift is more pronounced in the corresponding pyridinium–dichloroacetate complex indicating that pyridine is more basic than bipyridine.[15]

Proton transfer in bipyridinium–anion complexes

The mechanisms of proton transfer in the different bipyridinium–anion complexes arising from the above-mentioned findings are summarized in Scheme 5. Whereas the anions BF_4^- and AC^- lift the chemical equivalence of the two pyridine rings and, thus, quench the intramolecular transfer at low temperatures, $BARF^-$ does not effect remarkably the geometry of the intramolecular NHN hydrogen bond and thus enables the intramolecular proton transfer. A rough estimation of the rate constant of the intramolecular proton transfer can be obtained from the average ^{15}N signal at 120 K, Fig. 3d: $k = \pi\Delta\nu^2/2(W - W_0)$. The intrinsic linewidth W_0 of 35 Hz is estimated from Fig. 3a. The exchange broadening W of 45 Hz is estimated from Fig. 3d. The chemical shift difference $\Delta\nu$ can be assumed to be of about 100 ppm, that is 5000 Hz. Thus, we estimate that the rate constant k of the intramolecular proton transfer is of the order of 10^6 s^{-1}. The same value can be obtained using the line-shape analysis of the ^1H NMR spectrum at 130 K as described above, Fig. 2g. The latter analysis suggests that the exchange must be faster than 10^4 s^{-1}. These findings indicate little influence of $BARF^-$ on the hydrogen bond of $BpyH^+$ although the two might form a contact ion pair. This is probably the result of two features of $BARF^-$: (i) it has no tendency to form hydrogen bonds with proton donors and (ii) the electrical charge is well shielded and delocalized. We were not able to determine kinetic H/D isotope effects on the degenerate intramolecular proton transfer in $BpyH^+$ in order to obtain additional information about the mechanism of this process. For the isolated ion we expect a symmetric double-well potential for the proton motion, with a higher barrier as compared to the homoconjugated collidinium cation (Scheme 1d).[7] In polar solvents, the solvent molecules will exhibit at a given time an asymmetry of the hydrogen bond and localize the proton in one of the potential wells. Reorganization of the solvent shell is then required for proton transfer to occur.[28] The rate limiting step may then be the solvent reorganization.

In the case of the $BpyH^+$ BF_4^- complex both the Coulomb interaction as well as the hydrogen bond energy of $BpyH^+$ with BF_4^- will be substantially larger than with $BARF^-$. These intermolecular interactions hinder the intramolecular proton transfer. The line-shape analysis of the ^1H NMR spectrum at 130 K shows that the rate constant must be smaller than 10 s^{-1}, Fig. 2e. We expect that $BpyH^+$ BF_4^- must dissociate to allow the intramolecular proton transfer in the cation. Thereby, the dissociation is the rate-limiting step of the process.

The intermolecular interactions are even stronger with AC^-, as the basicity of AC^- is higher than of BF_4^-. The hydrogen

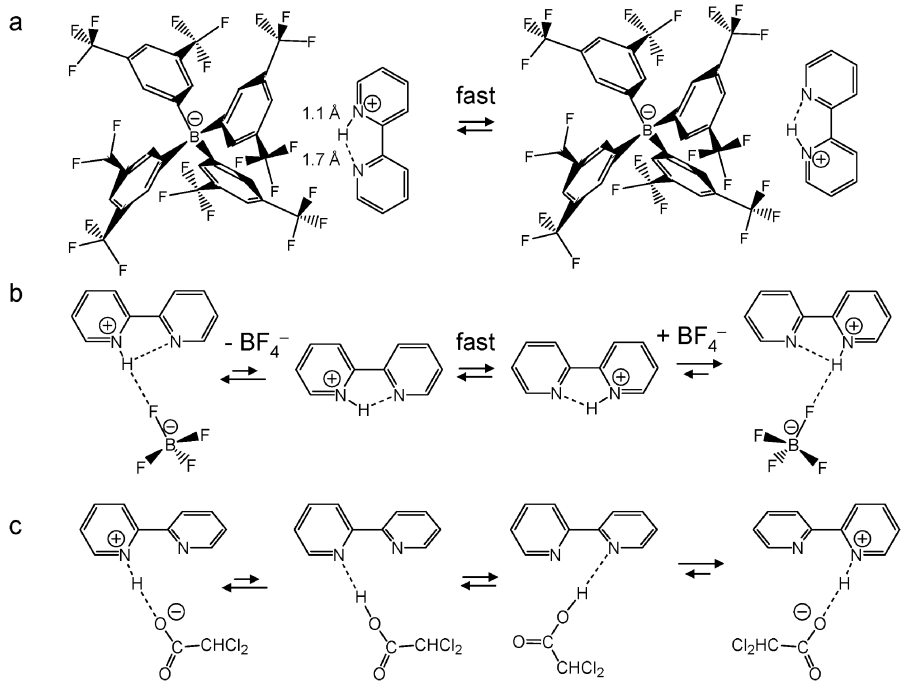

Scheme 5 Proton transfer in $BpyH^+$ anion complexes.

bonded proton signal of $BpyH^+$ AC^- consists of a broadened distorted triplet at 120 K or a broadened doublet at 115 K (Fig. 2b and c), indicating an intramolecular proton transfer which is fast on the ^1H but in view of the two ^{15}N signals (Fig. 3b) it is slow on the ^{15}N time scale. The analysis of the line shapes in Fig. 2b and c give rate constants of about 300 and 100 s^{-1} at 120 and 115 K, respectively. This is much slower than in $BpyH^+$ $BARF^-$, but also much faster than in $BpyH^+$ BF_4^-. The intermolecular interaction energy of the $BpyH^+$ AC^- complex is presumably large enough to prevent a dissociation of the ion pair at low temperatures. The observed intramolecular proton transfer may occur by a proton shift towards the acetate, followed by a hydrogen bond switch to the other nitrogen site and proton back-transfer. This mechanism resembles the tautomerism of diaryl-triazenes (Scheme 1b).[4]

Conclusions

In this study we have found using low-temperature NMR that the mechanism of the intramolecular proton transfer in 2,2′-bipyridinium cation depends principally on the charge distribution in the counteranion. Thus, $BpyH^+$ represents likely a unique example of three different counteranion-dependent mechanisms of intramolecular proton transfer observed in the same cation.

(i) The bulky $BARF^-$ does not exhibit a preferential interaction with one of the pyridine rings. Therefore, it lets bipyridinium to organize a strong intramolecular NHN hydrogen bond. A very fast degenerate intramolecular proton transfer was detected in $BpyH^+$ (Scheme 5a). A similar effect was detected before in the case of proton sponges (Scheme 1e),[12] but the difference to other anions was much less pronounced in the latter case.

(ii) There is a specific interaction between BF_4^- and $BpyH^+$ which quenches the intramolecular proton transfer as the ion pair needs to dissociate for this process to occur (Scheme 5b). This is in contrast to the homoconjugated collidinium cation where BF_4^- does not affect the formation of the intermolecular hydrogen bond (Scheme 1d).[6]

(iii) Bipyridinium forms a strong hydrogen bond with the very basic dichloroacetate AC^-. When temperature is increased, this hydrogen bond becomes stronger and a proton is shifted back from nitrogen towards the hydrogen bond center, as illustrated by a low-field shift of the hydrogen bond proton. It seems that the hydrogen bond and the associated Coulomb interaction are so strong that dissociation of the ion pair followed by an intramolecular proton transfer is not operative. However, a shift of the proton towards the anion and a subsequent hydrogen bond switch can explain the observed intramolecular proton transfer which is relatively slow.

In summary, the observations made in this study provide a model case of how nature controls function—here hydrogen bond and proton transfer phenomena—*via* a subtle interplay of chemical structure, conformation, and intermolecular interactions. This is of special importance in biomolecules. As some of us have shown recently, the protonation state of the cofactor vitamin B6 embedded in aspartate aminotransferase is better modeled using polar organic solvents rather than water,[29] the present study might be relevant to develop a detailed physical chemistry of active sites in biomolecules.

Acknowledgements

This work was supported by funds provided by the Deutsche Forschungsgemeinschaft, Bonn, the Fond der Chemischen Industrie, Frankfurt, the Russian Ministry of Education and Science (Project RNP 2.1.1. 485) and the Russian Foundation

of Basic Research (Project 09-03-91336). We thank Prof. G. S. Denisov (St. Petersburg State University, Russia) for stimulating discussions.

References

1 Z. Smedarchina, W. Siebrand, A. Fernandez-Ramos and Q. Cui, *J. Am. Chem. Soc.*, 2003, **125**, 243–251; Z. Smedarchina, A. Fernandez-Ramos and W. Siebrand, *J. Comput. Chem.*, 2001, **22**, 787–801; Z. Smedarchina, W. Siebrand, A. Fernandez-Ramos, L. Gorb and J. Leszczynski, *J. Chem. Phys.*, 2000, **112**, 566–573.

2 S. T. Arroyo, A. H. Garcia and J. A. S. Martin, *Chem. Phys.*, 2008, **353**, 73–78; *Hydrogen—Transfer Reactions*, ed. J. T. Hynes, H. H. Limbach and R. L. Schowen, Weinheim, Wiley-VCH, 2007, vol. 1–4; S. T. Arroyo, A. H. Garcia and J. A. S. Martin, *Chem. Phys.*, 2003, **293**, 193–202; J. Waluk, *Acc. Chem. Res.*, 2003, **36**, 832–838.

3 J. M. Lopez del Amo, U. Langer, V. Torres, G. Buntkowsky, H. M. Vieth, M. Pérez-Torralba, D. Sanz, R. M. Claramunt, J. Elguero and H. H. Limbach, *J. Am. Chem. Soc.*, 2008, **130**, 8620–8632.

4 H. H. Limbach, F. Männle, C. Detering and G. S. Denisov, *Chem. Phys.*, 2005, **319**, 69–92.

5 J. Braun, R. Schwesinger, P. G. Williams, H. Morimoto, D. E. Wemmer and H. H. Limbach, *J. Am. Chem. Soc.*, 1996, **118**, 11101–11110.

6 P. Schah-Mohammedi, I. G. Shenderovich, C. Detering, H.-H. Limbach, P. M. Tolstoy, S. N. Smirnov, G. S. Denisov and N. S. Golubev, *J. Am. Chem. Soc.*, 2000, **122**, 12878–12879.

7 B. Chen and J. E. Del Bene, *Mol. Phys.*, 2009, **107**, 1095–1105; B. Chen and J. E. Del Bene, *J. Am. Chem. Soc.*, 2007, **129**, 12197–12199; I. G. Shenderovich, *Russ. J. Gen. Chem.*, 2007, **77**, 620–624.

8 A. Szemik-Hojniak, I. Deperasińska, W. J. Buma, G. Balkowski, A. F. Pozharskii, N. V. Vistorobskii and X. Allonas, *Chem. Phys. Lett.*, 2005, **401**, 189–195; A. J. Bienko, Z. Latajka, W. Sawka-Dobrowolska, L. Sobczyk, V. A. Ozeryanskii, A. F. Pozharskii, E. Grech and J. Nowicka-Scheibe, *J. Chem. Phys.*, 2003, **119**, 4313–4319; I. Alkorta and J. Elguero, *Struct. Chem.*, 2000, **11**, 335–340.

9 D. Henschel, O. Moers, I. Lange, A. Blaschette and P. G. Jones, *Z. Naturforsch. B: J. Chem. Sci.*, 2002, **57**, 777–790; R. J. Bowen, M. A. Fernandes, P. W. Gitari and M. Layh, *Acta Crystallogr., Sect. C: Cryst. Struct. Commun.*, 2004, **60**, o113–O114; I. A. Guzei, J. Roberts and D. A. Saulys, *Acta Crystallogr., Sect. C: Cryst. Struct. Commun.*, 2002, **58**, m141–m143.

10 F. E. Kuhn, M. Groarke, E. Bencze, E. Herdweck, A. Prazers, A. M. Santos, M. J. Calhorda, C. C. Romao, I. S. Goncalves, A. D. Lopes and M. F. Pillinger, *Chem.–Eur. J.*, 2002, **8**, 2370–2383; G. B. Ma, A. Ilyukhin and J. Glaser, *Acta Crystallogr. Sect. C*, 2000, **56**, 1473–1475.

11 S. T. Howard, *J. Am. Chem. Soc.*, 1996, **118**, 10269–10274; A. Hazell, *Polyhedron*, 2004, **23**, 2081–2083; J. Kalenik and Z. Pawelka, *J. Mol. Liq.*, 2005, **121**, 63–68.

12 M. Pietrzak, J. P. Wehling, S. Kong, P. M. Tolstoy, I. G. Shenderovich, C. López, R. M. Claramunt, J. Elguero, G. S. Denisov and H. H. Limbach, *Chem.–Eur. J.*, 2010, **16**, 1679–1690.

13 N. S. Golubev, S. N. Smirnov, P. Schah-Mohammedi, I. G. Shenderovich, G. S. Denisov, V. A. Gindin and H.-H. Limbach, *Russ. J. Gen. Chem.*, 1997, **67**, 1082–1088.

14 R. P. Taylor and I. D. Kuntz Jr, *J. Am. Chem. Soc.*, 1972, **94**, 7963–7965.

15 S. N. Smirnov, N. S. Golubev, G. S. Denisov, H. Benedict, P. Schah-Mohammedi and H. H. Limbach, *J. Am. Chem. Soc.*, 1996, **118**, 4094–4101.

16 I. G. Shenderovich, A. P. Burtsev, G. S. Denisov, N. S. Golubev and H. H. Limbach, *Magn. Reson. Chem.*, 2001, **39**, S91–S99; S. Sharif, I. G. Shenderovich, L. González, G. S. Denisov, D. N. Silverman and H. H. Limbach, *J. Phys. Chem. A*, 2007, **111**, 6084–6093.

17 T. W. Whaley and D. G. Ott, *J. Labelled Compd.*, 1974, **10**, 283–286; A. I. Vogel, in *Vogel's Textbook of Practical Organic Chemistry*, Prentice Hall, 5th-edn, 1989, ch. 6, pp. 884–885; C. F. H. Allen and J. R. Thirtle, in *Organic Syntheses*, ed. E. C. Horning, WILEY, 1966, vol. 3, pp. 136–138.

18 S. Hayashi and K. Hayamizu, *Bull. Chem. Soc. Jpn.*, 1991, **64**, 685–687; M. Witanowski, L. Stefaniak, S. Szymański and H. Januszewski, *J. Magn. Reson.*, 1977, **28**, 217–226.

19 H. J. Reich, J. Chem. Educ. Software 3D2.

20 H. H. Limbachin *NMR Basic Principles and Progress*, Springer-Verlag, Heidelberg, 1991, vol. 23, pp. 66–167.

21 R. M. Claramunt, D. Sanz, S. H. Alarcón, M. Pérez-Torralba, J. Elguero, C. Foces-Foces, M. Pietrzak, U. Langer and H. H. Limbach, *Angew. Chem., Int. Ed.*, 2001, **40**, 420–423; M. Pietrzak, H. H. Limbach, M. Pérez-Torralba, D. Sanz, R. M. Claramunt and J. Elguero, *Magn. Reson. Chem.*, 2001, **39**, S100–S108.

22 D. V. Andreeva, B. Ip, A. Gurinov, P. M. Tolstoy, G. S. Denisov, I. G. Shenderovich and H. H. Limbach, *J. Phys. Chem. A*, 2006, **110**, 10872–10879.

23 J. E. Del Bene, I. Alkorta and J. Elguero, *J. Phys. Chem. A*, 2009, **113**, 12411–12420.

24 H. H. Limbach, M. Pietrzak, H. Benedict, P. M. Tolstoy, N. S. Golubev and G. S. Denisov, *J. Mol. Struct.*, 2004, **706**, 115–119.

25 P. Lorente, I. G. Shenderovich, N. S. Golubev, G. S. Denisov, G. Buntkowsky and H. H. Limbach, *Magn. Reson. Chem.*, 2001, **39**, S18–S29.

26 H. H. Limbach, M. Pietrzak, S. Sharif, P. M. Tolstoy, I. G. Shenderovich, S. N. Smirnov, N. S. Golubev and G. S. Denisov, *Chem.–Eur. J.*, 2004, **10**, 5195–5204.

27 I. G. Shenderovich, *Russ. J. Gen. Chem.*, 2006, **76**, 501–506.

28 C. L. Perrin, *Pure Appl. Chem.*, 2009, **81**, 571–583; C. L. Perrin and P. Karri, *Chem. Commun.*, 2010, **46**, 481–483.

29 S. Sharif, E. Fogle, M. D. Toney, G. S. Denisov, I. G. Shenderovich, P. M. Tolstoy, M. Chan Huot, G. Buntkowsky and H. H. Limbach, *J. Am. Chem. Soc.*, 2007, **129**, 9558–9559.